Circadian miR-449c-5p regulates uterine Ca2+ transport during eggshell calcification in chickens

Zhifu Cui
Sichuan Agricultural University
Zhichao Zhang
Sichuan Agricultural University
Felix Kwame Amevor
Sichuan Agricultural University
Xiaxia Du
Sichuan Agricultural University
Liang Li
Sichuan Agricultural University
Yaofu Tian
Sichuan Agricultural University
Xincheng Kang
Sichuan Agricultural University
Gang Shu
Sichuan Agricultural University
Qing Zhu
Sichuan Agricultural University
Yan Wang
Sichuan Agricultural University
Diyan Li
Sichuan Agricultural University
Yao Zhang
Sichuan Agricultural University
Xiaoling Zhao (zhaoxiaoling@sicau.edu.cn)
Sichuan Agricultural University

Research Article

Keywords: Chicken uterine, Circadian miRNAs, Tubular gland cells, Ca 2+ transport

Posted Date: March 15th, 2021

DOI: https://doi.org/10.21203/rs.3.rs-213129/v2

Circadian miR-449c-5p regulates uterine Ca^{2+} transport during eggshell calcification in chickens

Zhifu Cui[1], Zhichao Zhang[1], Felix Kwame Amevor[1], Xiaxia Du[1], Liang Li[1], Yaofu Tian[1], Xincheng Kang[1], Gang Shu[2], Qing Zhu[1], Yan Wang[1], Diyan Li[1], Yao Zhang[1], Xiaoling Zhao[1*]

Zhifu Cui and Zhichao Zhang have equal contribution to this paper.

1. Farm Animal Genetic Resources Exploration and Innovation Key Laboratory of Sichuan Province, Sichuan Agricultural University, Chengdu 611130, China.
2. Department of Pharmacy, College of Veterinary Medicine, Sichuan Agricultural University, Chengdu, Sichuan Province, P. R. China.

* Corresponding author:

Xiaoling Zhao, Department of Animal Science, Sichuan Agricultural University, Apt 211, Huimin Road, Wenjiang District, Chengdu, Sichuan Province, P. R. China. Zip code: 611130. E-mail: zhaoxiaoling@sicau.edu.cn.

Abstract

Background: miRNAs regulate circadian patterns by modulating animal biological clock. Clock genes exhibited a cosine expression pattern in the fallopian tube of chicken uterus in our previous study. Clock-controlled miRNAs are present in mammals and *Drosophila*; however, whether there are clock-controlled miRNAs in chicken uterus and, if so, how they regulate egg-laying rhythms are not clear. Here, we selected 18 layer hens with similar ovipositional rhythmicity (three birds were sacrificed for study per at 4 h intervals throughout 24 h); their transcriptomes were scanned to identify the circadian miRNAs and to explore regulatory mechanisms within the uterus of chickens.

Results: We identified six circadian miRNAs mainly associated with several biological processes including ion trans-membrane transportation, response to calcium ion, and enrichment of calcium signaling pathways. Verification of experimental results revealed that miR-449c-5p exhibited a cosine expression pattern in chicken uterus. Ca^{2+}-transporting ATPase 4 (*ATP2B4*) in the plasma membrane is the predicted target gene of circadian miR-449c-5p and is highly enriched in the calcium signaling pathway. We speculated that clock-controlled miR-449c-5p regulated Ca^{2+} transportation during eggshell calcification in chicken uterus by targeting *ATP2B4*. ATP2B4 mRNA and protein were rhythmically expressed in chicken uterus, and dual-luciferase reporter gene assays confirmed that ATP2B4 was directly targeted by miR-449c-5p. miR-449c-5p showed an opposite expression profile with ATP2B4 within a 24h cycle in chicken uterus; it inhibited mRNA and protein expressions of ATP2B4 in uterine tubular gland cells. Additionally, overexpression of *ATP2B4* significantly decreased intracellular Ca^{2+} concentration ($P < 0.05$), while knockdown of *ATP2B4* accelerated intracellular Ca^{2+} concentrations. Similar results were found after *ATP2B4* knockdown by miR-449c-5p. These results indicated that ATP2B4 promoted uterine Ca^{2+} trans-epithelial transport.

Conclusions: Clock-controlled miR-449c-5p regulates Ca^{2+} transport in chicken uterus by targeting ATP2B4 during eggshell calcification.

Keywords: Chicken uterine, Circadian miRNAs, Tubular gland cells, Ca^{2+} transport

Background

Animals physiology is dependent upon circadian clocks [1] located in the peripheral tissues for the maintenance of temporal order [2-5]. The master clock is situated in the suprachiasmatic nucleus (SCN) and many peripheral tissues involved in these clock cycles are known as oscillators [2-5]. Specific oscillators that are associated with circadian clocks are categorized as circadian oscillators [6]. Expression of these circadian oscillators takes place within approximate 24 h periods, which ultimately form the circadian biological clock [6]. Molecular clockworks modulate circadian rhythms in every cell that is controlled by circadian genes and proteins via transcriptional-translational feedback loop circulation [7, 8]. Researchers have previously identified CLOCK and BMAL1 as the basic helix-loop-helix (bHLH)-containing transcription factors and they play important roles in oscillator loops [9-12]. For instance, the CLOCK-BMAL1 complex is found in the mammalian circadian clockwork where it binds to the CACGTG E-box or its allied E-box-like sequence to promote rhythmic genes, regulate the transcription of those genes in peripheral tissues, and finally promote circadian oscillation [13-18]. Previous studies reported NPAS2 as a homologue of CLOCK; moreover, other vital clock homologous complexes such as CLOCK-BMAL1 or NPAS2-BMAL1 facilitate E-box-dependent transcription [19, 20]. NPAS2 is reported to compensate CLOCK [21-23]; therefore, any alterations in the form of deletions or mutations of NPAS2 could directly cause a complete disruption of biological rhythmical order [24].

MicroRNAs (miRNAs), from the family of ~22 nucleotide length and single-stranded non-coding RNA molecules, are known to regulate gene expression at the post-transcriptional level by targeting their 3′ untranslated regions (3′UTRs) [25, 26]. Studies confirm that miRNAs play specific regulatory roles in circadian rhythms. In mice, for instance, specific miRNAs such as miR-96, miR-124a, and miR-27b-3p have been found oscillating in a circadian pattern [27, 28]. Other miRNAs such as miR-206 in mammalian skeletal muscle [29], miR-219, miR-132 and miR-142-3p in mice [30, 31], miR-263a, miR-263b and let-7 in *Drosophila* [32, 33], miR-182 in humans with depression [34], and miR-17-5p and miR-29b-3p in rats [35] are widely reported.

Compared with other animals, birds have a more complex circadian system because its function requires pacemakers to be present in organs such as the pineal gland, retina, and SCN that

regulates peripheral tissues [6, 36]. Oscillators in the pineal gland and SCN are known to be functionally involved in stabilizing and amplifying each other through their periodic release of secretions [37]. Reports suggest that numerous physiological outputs such as the daily egg-laying rhythm in birds are influenced by coordination of circadian outputs through the various pacemakers present in the pineal gland and SCN [38, 39].

At peak egg production, chickens oviposit within 24～25 h cycles [40, 41], wherein a luteinizing hormone surge modulates the expression of genes related to the circadian clock [40]. Our previous study observed that the cosine expressions of clock genes are involved in the regulation of the circadian clock in the uterus of chicken's oviduct [41]. Other studies report the actions of specific clock miRNAs in mammals and *Drosophila*, however, there have been no reports in chickens. Therefore, in this study, we adopted RNA sequencing (RNA-seq) to identify clock-controlled miRNAs and explore their roles in signaling pathways in chicken uterus.

Results

Morphological and histological characteristics of chicken uterus

Results of the morphological or physical observations of the oviducts showed that eggs were present in the oviduct ampulla and isthmus at ZT4 and ZT8, respectively; whereas eggs were present in the uterus at ZT12, ZT16, ZT20 and ZT0. According to histological observations, we found the uterine glands in the endometrium had a folded and branched tubular structure. The density of uterine glands increased gradually from ZT0 to ZT12 and decreased from ZT12 to ZT20. Importantly, at ZT12, the endometrium thickened, and both the length and folding of the uterine glands increased (Fig. 1). Moreover, the number of tubular gland cells increased and were neatly arranged; these secreted the uterine fluid containing various ions such as K^+, Na^+, HCO^{3-}, and Ca^{2+} [42]. This may increase the contact area between uterine tubular gland cells and the egg to rapidly secrete large amounts of uterine fluid.

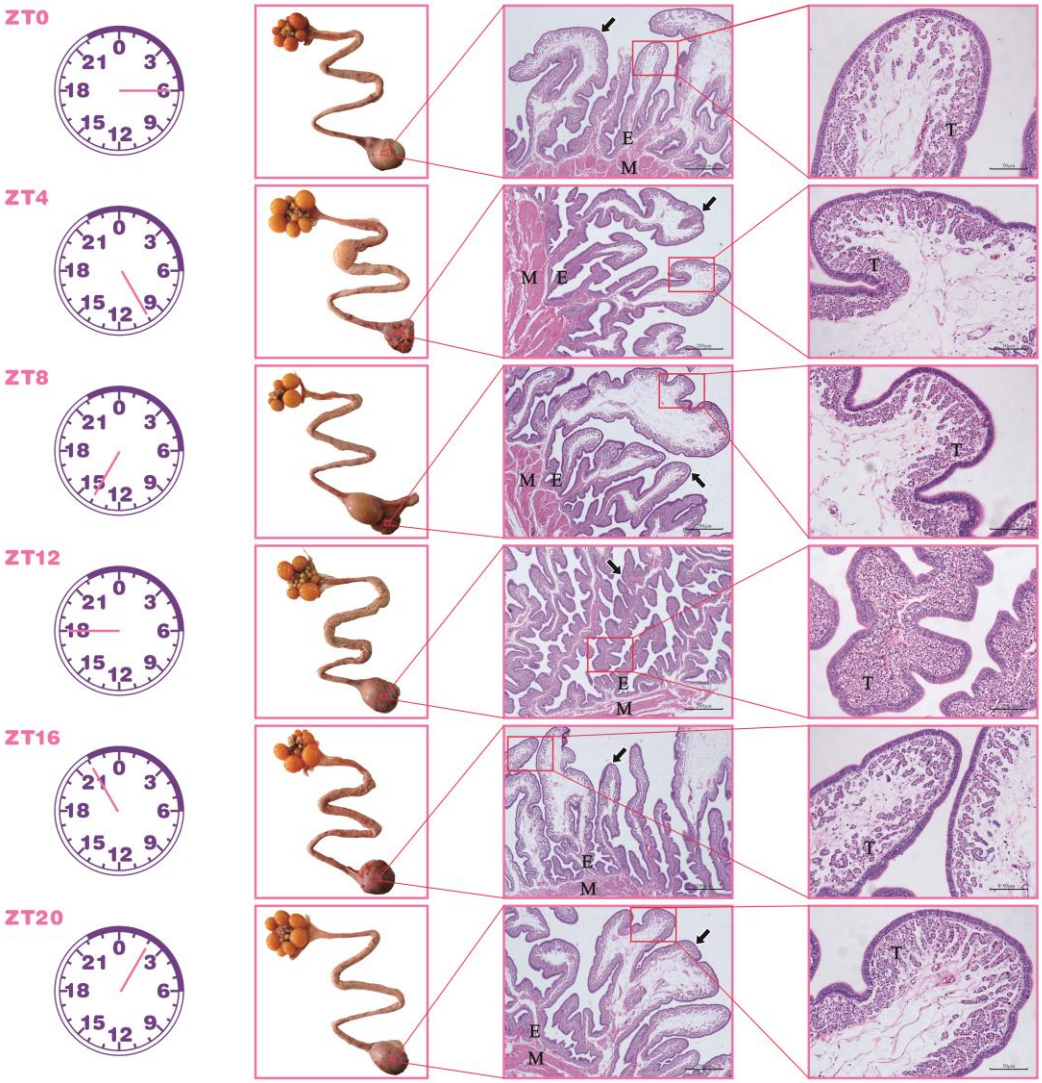

Fig. 1 Chicken uterus morphological and histological characteristics. Hematoxylin-eosin (H&E) staining of chicken uterus at ZT4, ZT8, ZT12, ZT16, ZT20, and ZT0 (ZT24), respectively (magnified 200×). Replications = 3. E: endometrium; M: myometrium; T: tubular gland cells. The black arrow indicates the endometrial glands.

Identification of circadian miRNAs and miRNA-gene interaction network

The miRNAs expressed in the uterine tissues were calculated and plotted as heatmaps (Fig. 2A). In general, six miRNAs were identified as circadian miRNAs in the uterus (Fig. 2B), and then a core clock genes-miRNAs correlation network (Fig. 2C) and a circadian miRNAs-target genes correlation network (Fig. 2D) were constructed. The results of the target genes of the 6 circadian miRNAs and uterus cyclical genes (our recently submitted uterus mRNA sequencing data) (PRJNA699682) are presented in a Venn diagram. GO and KEGG pathway analyses were performed on a total of 127 circadian target genes (Fig. 2E). The top 15 terms were involved in

biological functions such as regulation of ion transmembrane transport, regulation of sodium ion transmembrane transporter activity, response to calcium ion, negative regulation of release of sequestered calcium ion into cytosol, cellular response to carbon dioxide, and positive regulation of endothelial cell migration (Fig. 2F). KEGG analysis showed that these circadian target genes were enriched in the calcium signaling pathway, endocytosis, metabolic pathways, MAPK signaling pathway, regulation of actin cytoskeleton, nitrogen metabolism, cell cycle, TGF-beta signaling pathway, ether lipid metabolism, and FoxO signaling pathway (Fig. 2G). The target genes of clock-controlled miRNAs involved in the ion transfer during eggshell calcification are summarized in Table 2.

Table 2 Target genes of clock-controlled miRNAs involved in ion transfer during eggshell calcification.

miRNAs	**Target genes**	**Transfer type**
gga-miR-218-5p	NPAS2, CA2	Catalyse HCO_3^- formation (plasma membrane)
	KCNH1/5/7	Inward rectifiers K^+ channels (plasma membrane)
gga-miR-449c-5p	ATP2B4	Ca^{2+}/H^+ exchanger (plasma membrane)
	FKBP1A/B	Ca^{2+} channel (endoplasmic membrane)
gga-miR-34b-5p	ATP2B4	Ca^{2+}/H^+ exchanger (plasma membrane)
gga-miR-1727	TRPV4/5	Ca^{2+} channel (plasma membrane)
gga-miR-32-3p	KCNH1	Inward rectifiers K+ channels (plasma membrane)
	SLC4A7	Na^+/HCO_3^- co-transporters (plasma membrane)

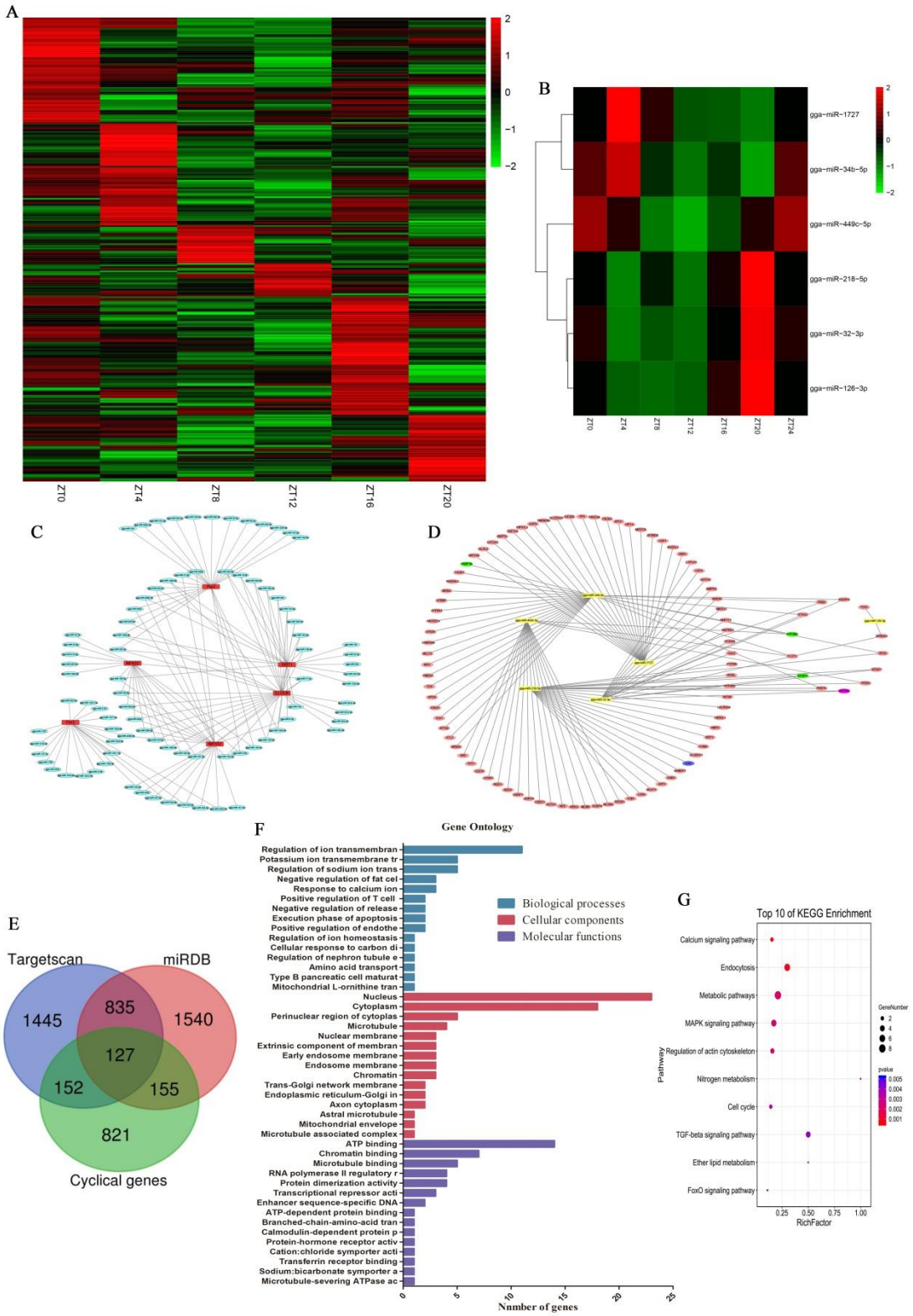

Fig. 2 Identification of circadian miRNAs and functional analysis. (A) Heatmap of a total of 375 miRNAs in chicken uterus at ZT4, ZT8, ZT12, ZT16, ZT20, and ZT0 (ZT24) within 24 h. (B) Heatmap of six circadian miRNAs. (C) Core clock genes-miRNAs correlation network in chicken uterus. (D) Circadian miRNAs-target genes correlation network in chicken uterus. (E) Venn diagram showing the target genes of six circadian miRNAs using Targetscan and miRDB software, and uterine cyclical genes. (F) GO enrichment of the 127 circadian target genes. Top 15 terms of

biological process, cellular component, and molecular function. X-axis shows the number of genes. (G) Top 10 significantly enriched pathways associated with 127 circadian target genes.

Clock-controlled miR-449c-5p modulated ATP2B4 expression

The results from Targetscan software prediction analysis showed that the seed region of miR-449c-5p was complementary to the 3′-UTR of the *ATP2B4* gene (Fig. 3A). Moreover, after the expression abundances of miR-449c-5p and *ATP2B4* at different time points within a 24 h cycle in uterine tissues were determined, we found a reduction in the expression level of miR-449c-5p from ZT0 to ZT12; however, it eventually increased from ZT12 to ZT20 (Fig. 3B). Contrarily, the mRNA expression of *ATP2B4* increased, reached its highest level at ZT12, and then decreased sharply (Fig. 3C). Dual-luciferase reporter gene assay results showed that luciferase activities of the ATP2B4 wild-type reporter vector decreased significantly with response to miR-449c-5p mimic while no dramatic changes were observed in its mutant vector (Fig. 3D); these results indicated that *ATP2B4* is a target gene of miR-449c-5p.

To investigate the function of miR-449c-5p on Ca^{2+} transfer in the uterus, immunofluorescence analysis was performed to identify uterine tubular gland cells. Cytokertin 18 (CK18) is a specific cytokeratin uterine tubular gland cell marker [43, 44]. Immunofluorescence analysis showed that the cells isolated and cultured were chicken uterine tubular gland cells (Fig. 3E). miR-449c-5p expression increased significantly after it was transfected with miR-449c-5p mimic ($P < 0.05$) (Fig. 3F), but its expression decreased after transfection with miR-449c-5p inhibitor (Fig. 3G).

The mRNA and protein levels of ATP2B4 decreased significantly due to the overexpression of miR-449c-5p (Fig. 3H, J, and K), whereas the results obtained after the inhibition of miR-449c-5p showed that the mRNA and protein expressions of ATP2B4 increased significantly (Fig. 3I, J, and K). Immunohistochemistry showed that the protein expression of ATP2B4 in the uterus increased first and then gradually reduced from ZT0 to ZT20 with the highest at ZT12 (Fig. 4A and B), which was similar to the trend of mRNA expression of *ATP2B4*.

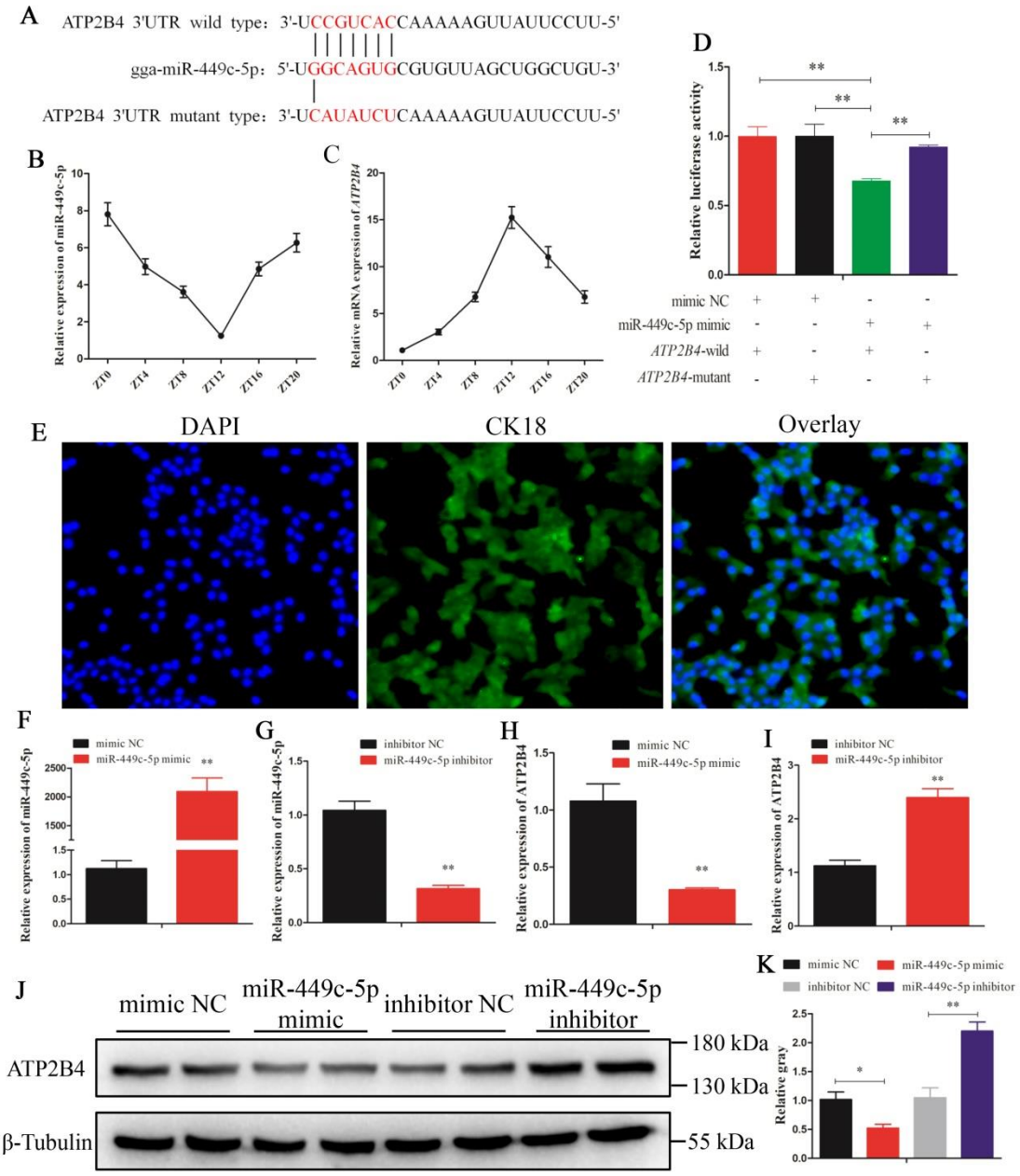

Fig. 3 Clock-controlled miR-449c-5p inhibited ATP2B4 mRNA and protein expression by directly targeting ATP2B4 in uterine tubular gland cells. (A) The target position of the miR-449c-5p seed sequence on the gene ATP2B4-3′UTR sequence (red characters) was predicted by TargetScan software. (B, C) Relative expression of miR-449c-5p and ATP2B4 at the time point of ZT0 (ZT24), ZT4, ZT8, ZT12, ZT16, and ZT20 in chicken uterus, respectively. (D) Chicken DF-1 cells were co-transfected with ATP2B4-3′UTR wild or mutant dual-luciferase vector and the miR-449c-5p mimic or mimic-NC. The relative luciferase activity was assayed 48h later. (E) Immunofluorescence analysis was performed to identify the uterine tubular gland cells. (F, G) qRT-PCR was used to determine the miR-449c-5p expression levels after transfection of miR-449c-5p overexpression and miR-449c-5p inhibition plasmid, respectively. (H, I) mRNA expression of ATP2B4 in chicken uterine tubular gland cells was detected by qRT-PCR after overexpression and inhibition of miR-449c-5p, respectively. (J, K) Protein expression of ATP2B4 in chicken uterine tubular gland cells was detected by Western blot analysis after a gain or loss of

miR-449c-5p, respectively. UTR: untranslated region; miR: microRNA; DAPI: 4′, 6-diamidino-2-phenylindole; NC: negative control. Replications = 3. The samples derive from the same experiment and that gels/blots were processed in parallel. The data is presented as mean ± standard error (SE); *P < 0.05 and **P < 0.01.

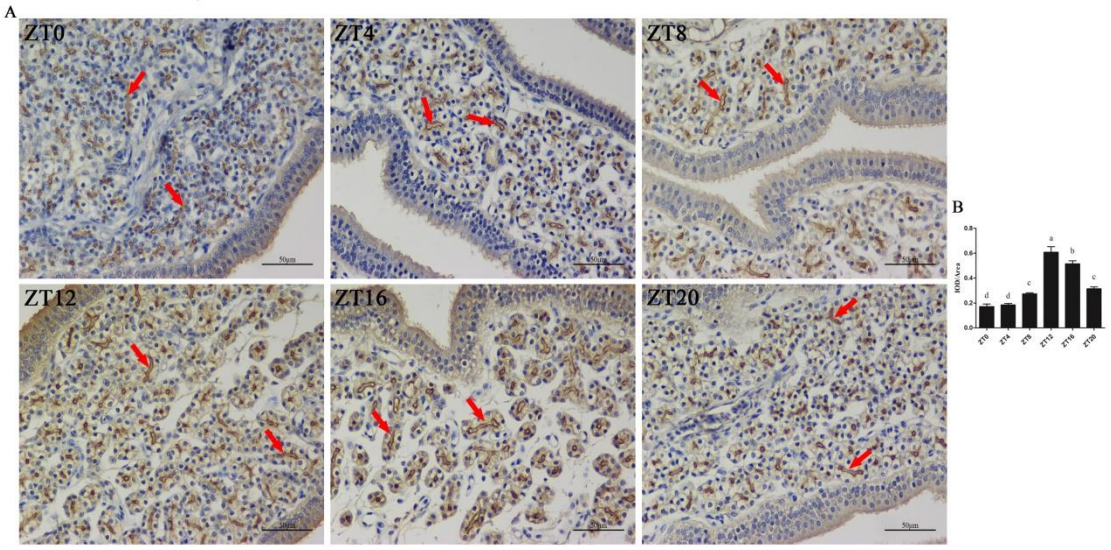

Fig. 4 ATP2B4 immunohistochemistry in the chicken uterus. (A) Immunohistochemical staining with the ATP2B4 antibody visualized using chromogen diaminobenzene (brown staining) in the chicken uterus. Arrows indicate the relative areas of positive staining. (B) Digital conversion histogram; each point represents the mean ± SE. Different lowercase letters indicate a significant difference among groups (P < 0.05).

ATP2B4 regulated Ca^{2+} transfer in uterine tubular gland cells

The mRNA and protein abundances of ATP2B were determined after transfection with pcDNA3.1-ATP2B4 and pcDNA3.1 empty plasmid, or Si-ATP2B4 and Si-NC. Compared with group pcDNA3.1, group pcDNA3.1-ATP2B4 significantly increased the mRNA and protein levels of ATP2B4 (Fig. 5A, B, and C). Meanwhile, group Si-ATP2B4 had lower mRNA and protein levels of ATP2B4 than group Si-NC (Fig. 5D, E, and F). Compared with the control group (mimic NC), overexpression of miR-449c-5p significantly increased the fluorescence value after transfection for 24 h, indicating an increase in intracellular Ca^{2+} concentration (Fig. 5G). A knockdown of miR-449c-5p reduced the concentration of Ca^{2+} (Fig 5H). Moreover, *ATP2B4* overexpression significantly decreased the concentration of Ca^{2+} after transfection for 24 h and 36 h (Fig. 5I), respectively. These results are similar to the down-regulation of miR-449c-5p, but contrary to the knockdown of *ATP2B4* (Fig. 5J). Fluorescence intensity was significantly higher in the miR-449c-5p overexpression (Fig. 6A and B) and Si-ATP2B4 (Fig. 6G and H) groups, compared with the mimic NC and Si-NC groups, respectively. However, there was decreased fluorescence

intensity in the miR-449c-5p knockdown (Fig. 6C and D) and *ATP2B4* overexpression groups (Fig. 6E and F). All results indicated that ATP2B4 regulated uterine Ca^{2+} trans-epithelial transport.

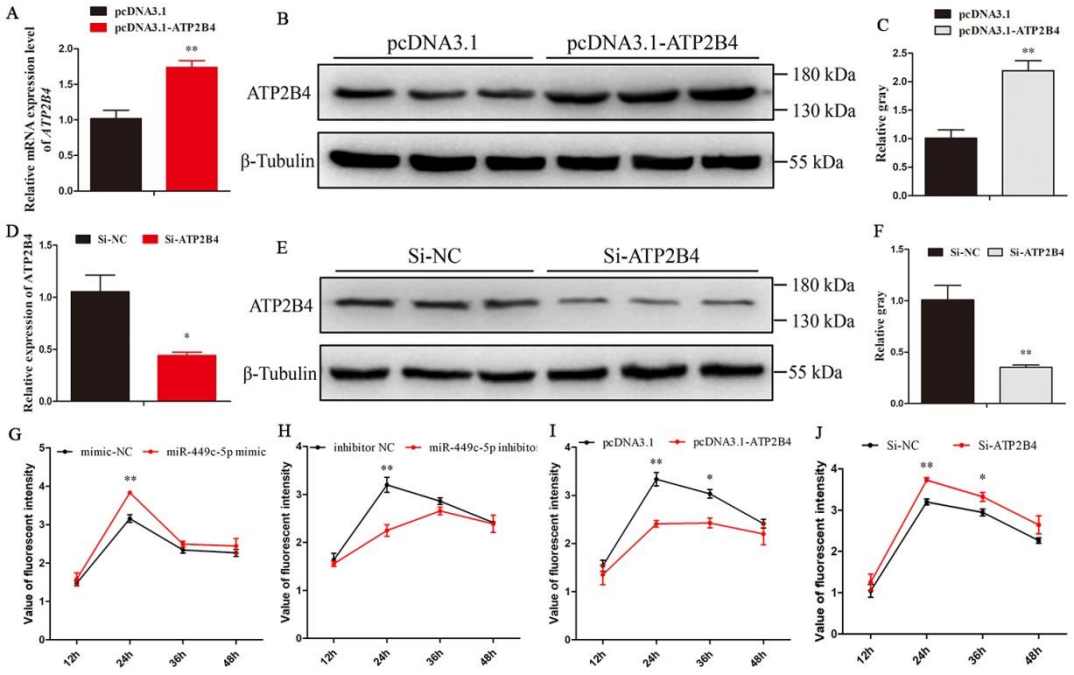

Fig. 5 ATP2B4 regulated Ca^{2+} transfer in uterine tubular gland cells. (A, B and C) mRNA and protein expressions of ATP2B4 were detected after transfection of overexpression plasmid (pcDNA3.1-ATP2B4) and empty pcDNA3.1 vector. (D, E, and F) mRNA and protein expressions of ATP2B4 were detected after transfection of small interfering RNA (Si-ATP2B4) and siRNA negative control (Si-NC). (G and H) Value of fluorescent intensity was measured using a microplate reader indicating the intracellular concentration of Ca^{2+} after overexpression and inhibition of miR-449c-5p. (I and J) The intracellular concentration of Ca^{2+} ion was detected after transfection overexpression and inhibition of ATP2B4. Replications = 3. The samples derive from the same experiment and that gels/blots were processed in parallel. Data are presented as mean ± standard error (SE); $*P < 0.05$ and $**P < 0.01$.

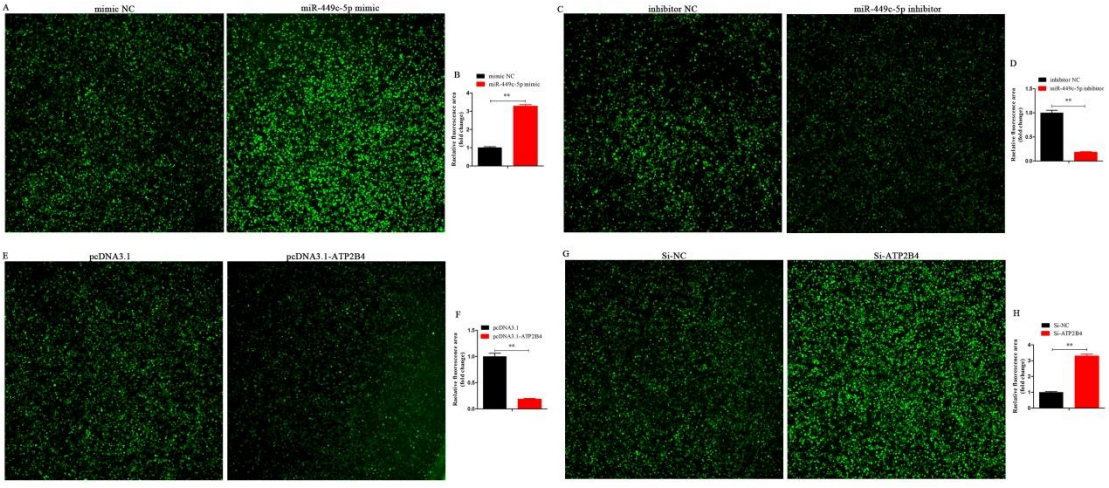

Fig. 6 Clock-controlled miR-449c-5p regulated Ca^{2+} transport by targeting ATP2B4 in chicken uterine tubular gland cells. (A and B) Fluorescence intensity was observed and analyzed after

overexpression of miR-449c-5p. (C and D) Fluorescence intensity was observed and analyzed after inhibition of miR-449c-5p. (E, F, G, and H) Fluorescence intensity was observed and analyzed after transfection, overexpression, and inhibition of ATP2B4. Replications = 3. Data are presented as mean ± standard error (SE); *P < 0.05 and **P < 0.01.

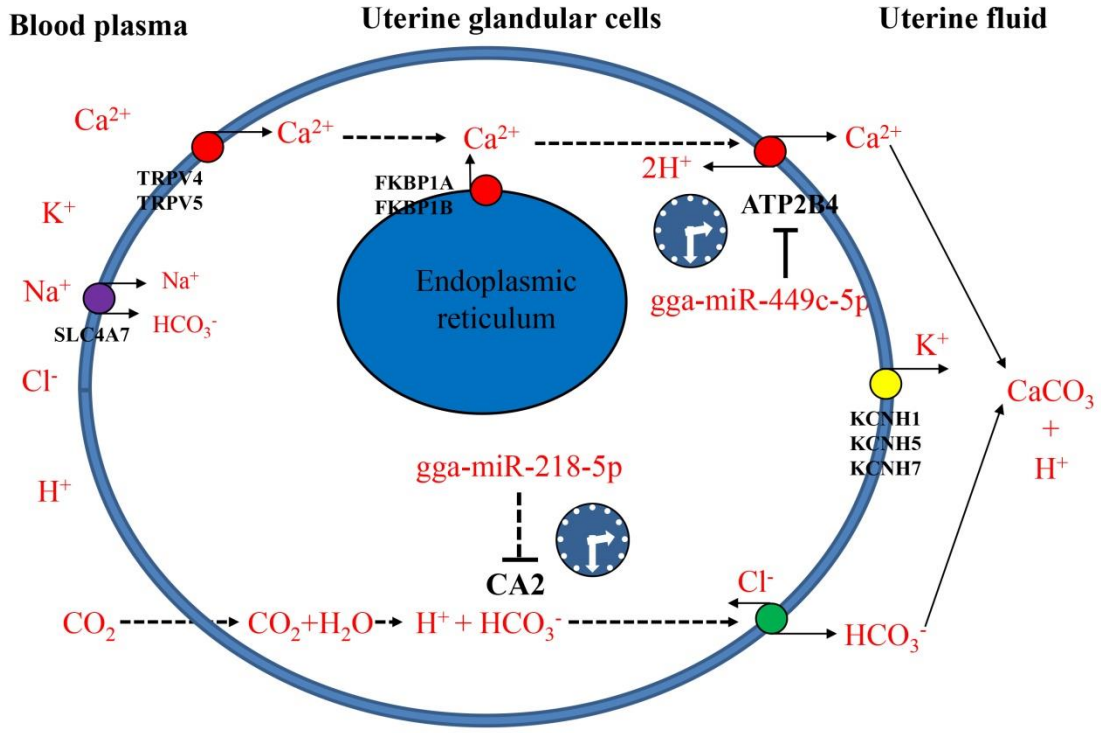

Fig. 7 The general model describing clock-controlled miRNA regulated ion transporters during eggshell calcification in the chicken uterus. This figure summarizes the general mechanisms involved in the regulation of the transport, distribution, and transformation of Ca^{2+} from the blood plasma through the uterine tubular gland cell membrane (Ca^{2+} trans-epithelial transport) and then suspended in the uterine fluid in a usable form ($CaCO_3$) to be utilized in eggshell calcification. Clock-controlled miR-449c-5p in the uterus of chickens regulated Ca^{2+} transport by targeting ATP2B4 during eggshell calcification. ATP2B4 was responsible for utilizing the stored energy in the form of ATP to extrude Ca^{2+} out of the cell against the electrochemical gradient and it was also involved in the active transport of calcium out of the tubular gland cells into the calcium-rich fluid of the uterine lumen. *NPAS2*, one of the core clock genes, was predicted to be the target gene of clock-controlled miR-218-5p, and another target gene *CA2*, was related to the carbonic anhydrase activity of the hen oviduct.

Discussion

The vital internal devices that run on an approximate 24 h cycle and respond to external rhythms through phase resetting are considered to be circadian clocks. Almost all living organisms possess circadian timekeeping mechanisms that help to monitor and regulate daily rhythms of physiological and behavioral activities [40, 41].

Chickens oviposit within a 24～25 h rhythm at peak egg laying periods. At this stage, clock genes in the oviduct exhibited cosine expression patterns [40, 41], which gives an indication that

238 the circadian clock plays a vital regulatory role in the chicken uterus. Cheng et al. report that
239 microRNAs regulate the circadian clock [30]. Therefore, to better understand the roles played by
240 specific miRNAs in eggshell calcification in the chicken uterus, we used transcriptome sequencing
241 to explore clock-controlled miRNA functions and their regulatory effects. The results revealed six
242 special clock-controlled miRNAs and their related pathways that play critical roles in eggshell
243 calcification in chicken uterus.

244 Shell calcification during egg formation requires the continuous supply of large amounts of
245 calcium and carbonate ions from the uterine fluid, which are derived from the blood stream via
246 trans-epithelial transport across the uterine gland cells [45, 46]. The developing egg is observed to
247 inflate and rotate in the uterus during the rapid phase of shell calcification (between 10 and 22 h
248 postovulation) [47]. In the present study, histological characteristics of the uterus showed that the
249 number of tubular gland cells increased as well as were neatly arranged at ZT12, which has been
250 reported as the time point for secretion of uterine fluid including various ions needed for eggshell
251 calcification [42]. From the results, we speculated that four hours before and after ZT12 is the
252 rapid phase of egg shell calcification in chicken.

253 There is a total reduction in the cellular functions resulting from a dysregulation or dysfunction
254 of miRNA(s). For instance, miR-449c-5p is reported to exhibit suppressive effects on the
255 osteogenic differentiation of valve interstitial cells. Hence, miR-449c-5p could be a potential
256 target for treating calcific aortic valve disease [48]. In this experiment, our results indicated that
257 the levels of miR-449c-5p in chicken uterus showed a pattern of cosine expression in the
258 verification experiment. This indicated that a biological clock regulated the miR-449c-5p. GO and
259 KEGG results showed that the target genes of these six circadian miRNAs were mainly associated
260 with biological processes including the regulation of ion transmembrane transport, response to
261 calcium ion, and calcium signaling pathway enrichment. Importantly, plasma membrane
262 Ca^{2+}-transporting ATPase 4 (ATP2B4) is a predicted target gene of clock-controlled miR-449c-5p
263 and is highly enriched in the calcium signaling pathway (Fig 7). A previous study localized
264 ATP2B4 in uterine tubular gland cells [49], and reported the promotion of trans-epithelial transfer
265 of Ca^{2+} into the uterine fluid in avian species [46]. We deduced that clock-controlled miR-449c-5p
266 may regulate Ca^{2+} transport during eggshell calcification in the chicken uterus.

267 In the cellular system, Ca^{2+} is regarded as one of the most important ions because of its active

involvement in cellular excitation and also serves as a vital second messenger. Hence, maintaining this electrochemical gradient is critical for normal cell physiological functioning and this requires an energy dependent mechanism of Ca^{2+} expulsion or conversion into a stable form ($CaCO_3$) [50]. In chickens, eggshell formation takes place daily in the uterus of oviduct and is one of the most rapid mineralization processes or physiological phenomena known [47]; during this process, large amounts of calcium carbonate ($CaCO_3$) are required. Neither of the involved elements (Ca^{2+} and HCO_3^-) are stored in the uterus but are continuously supplied during eggshell formation by the blood plasma via trans-epithelial transport which takes place across the uterine glandular cells [49, 51-55].

Plasma membrane calcium ATPases (ATP2Bs) are the main regulators of intracellular Ca^{2+} levels. Ca^{2+} secretion from the tubular gland cells is transported into the uterine fluid to actively form part of Ca^{2+}-ATPase [53, 55]. Plasma membrane Ca^{2+} ATPases are ubiquitously expressed in the plasma membrane and use ATP in the form of energy to pump Ca^{2+} out of the cells. In general, four paralogs ATP2B1, ATP2B2, ATP2B3, and ATP2B4 are found in the mammalian cells but only three (ATP2B1, B2, B4) are conserved in birds. These proteins are similar, but differ in tissue expression and speed of activation. The last step of uterine Ca^{2+} trans-epithelial transport is the output from the glandular cells, which occurs against a concentration gradient. Therefore, Ca^{2+} secretion towards the uterine fluid occurs via an active process, involving the Ca^{2+}-ATPase [55-57]. Plasma membrane calcium-transporting ATPase 4 (ATP2B4) is the coding subunit of plasma membrane Ca^{2+}-ATPase isoform 4 (PMCA4) [58]. Enzymes of PMCAs (ATP2B1, B2, B3, and B4) have been identified in mammals [59]. The activities and expressions of the Ca^{2+}-ATPase are associated with the periods of eggshell calcification especially when high concentrations of calcium ions are required for eggshell formation [55]. In this current study, we found that there was a rhythmical expression of the mRNA and protein levels of ATP2B4 and our confirmatory experiment affirmed that miR-449c-5p directly targeted ATP2B4. The results indicated that the expressions of miR-449c-5p were opposite to those for ATP2B4 within a 24 h cycle in the chicken uterus, and it was also revealed that miR-449c-5p inhibited mRNA and protein expressions of ATP2B4 in uterine tubular gland cells.

Previous reports describe ATP2B4 as the main mechanism found in the eggshell gland (ESG) of laying birds and is responsible for utilizing stored energy in the form of ATP to extrude Ca^{2+} out of

the cell against the electrochemical gradient [60, 61]. Another study identified and localized ATP2B4 in the uterine tubular gland cells of King Quail and confirmed its involvement in the active transport of calcium out of the tubular gland cells into the calcium-rich fluid of the uterine lumen [49]. In this study, we further explored the role of ATP2B4 in the transmembrane transport of calcium ions in the uterine tubular gland cells and found that *ATP2B4* overexpression significantly decreased the intracellular Ca^{2+} concentration but significantly increased with the transfection of *ATP2B4* knockdown, indicating that ATP2B4 promoted uterine Ca^{2+} trans-epithelial transport. Furthermore, miR-449c-5p showed similar changes on Ca^{2+} concentration with knockdown of *ATP2B4*, which were contrary to *ATP2B4* overexpression.

Conclusions

In conclusion, we identified six circadian miRNAs in the chicken uterus within a 24 h cycle. GO and KEGG analyses showed that the target genes were mainly associated with biological processes including: the regulation of ion transmembrane transport, response to calcium ion, and calcium signaling pathway enrichment. Therefore, we suggest that clock-controlled miR-449c-5p in chicken uterus regulated Ca^{2+} transport by targeting ATP2B4 during eggshell calcification (Fig. 7).

Methods

Animals

A total of 500 30-week-old laying hens (Line BH-01, bred by Sichuan Agriculture University for six generations with black shanks and dotted yellow feathers) were raised under a photoperiod of 16 h of light and 8 h of darkness (16L: 8D). Their oviposition time was monitored and recorded every 30 min from 06:00 h to 16:00 h. Zeitgeber time (ZT) is the nomenclature for time in light-dark cycle. The light in the chicken's pen was turned on at 06:00 h and turned off at 20:00 h. Illumination was provided by one row of un-shaded incandescent lamps (25 Watts); the mean luminance at a height of 2 m was 15 Lux. ZT0 (06:00 h) was the time at which the lamps were turned on, and subsequent times of light simulation lasted were denoted as ZT4 (10:00 h), ZT8 (14:00 h), ZT12 (18:00 h), ZT16 (22:00 h), and ZT20 (02:00 h), respectively.

Sample collection and RNA extraction

Eighteen hens with similar oviposition time were sacrificed at ZT4, ZT8, ZT12, ZT16, ZT20, and

ZT0 (ZT24) (three birds at successive 4-h intervals) by cervical dislocation and their uterine tissues were collected. All uterine samples were quickly frozen in liquid nitrogen and further stored at -80℃ until assayed for RNA and qRT-PCR analyses.

Morphological observation and histological staining

The uterine tissues were cut into sections and were embedded in paraffin for 24 h for further observation of morphological changes. Thereafter, sections were stained with hematoxylin and eosin (H&E) for observation under a fluorescence microscope (DP80; Olympus, Japan); 10 fields were randomly selected for statistical analysis.

Library construction and RNA-Seq

Total RNA was isolated from uterine tissues using TRIzol Reagent (Invitrogen, CA, USA) following the manufacturer's protocol. We determined the concentration and purity of RNA samples, and the integrity of 18S and 28S rRNA bands using A260/280 absorbance ratio and 2% agarose gel electrophoresis respectively. The cDNA libraries of small RNAs were generated using a Truseq^{TM} RNA sample prep kit (Illumina) according to the manufacturer's instructions and RNA sequencing was performed with an Illumina Hiseq 2500 system (Denovo Gene, Guangzhou, China).

Identification of circadian miRNAs

The R software package was used to identify the circadian miRNAs through JTK_CYCLE analysis as previously described [62]. Results of JTK_CYCLE analysis were represented as Q-value, *P*-value, and PER period value. Whereas the *P* and Q values denote the significance of miRNA rhythmic expression, the PER value stands for the rhythm cycle time. The miRNAs with both Q- and *P*-values < 0.05 and a periodic PER value of 20–24 were considered as candidate circadian miRNAs.

Bioinformatics analysis

In this study, we filtered the raw reads to obtain clean reads as previously described [63]. The miRNAs expressed were calculated and plotted in the heatmaps (R software v.3.2.4.). Thereafter, we constructed a regulatory interaction network between clock-controlled miRNAs and their target genes using integrative miRNA target-prediction (http://www.targetscan.org/vert_72/ and http://mirdb.org/index.html) [64] and network-analysis (Cytoscape software) [65]. We further conducted Gene ontology (GO) and Kyoto Encyclopedia of Genes and Genomes (KEGG)

pathway enrichment analysis to identify the biological functions of the target genes.

Dual-luciferase reporter assay

Chicken embryo fibroblast cell line (DF-1) were seeded in 48-well cell plates and cultured with growth medium containing F12 (Hyclone, State of Utah, USA) + 10% fetal bovine serum (Gibco, Langley, OK) in a cell culture incubator at 37 ℃, 5% CO_2 and 95% air saturated humidity. Reaching a cell density coverage of 70~80%, the plasmid (ATP2B4-3′UTR wild type or mutant type) was co-transfected with mimic negative control (NC) and miR-449c-5p respectively. Later (after 48 h), luciferase activity was tested using a luciferase reporter assay kit (Promega, Madison, WI, USA) following the manufacturer's instructions.

Immunohistochemical analysis

Uterine samples were collected at these time points ZT4, ZT8, ZT12, ZT16, ZT20, and ZT24, respectively, and were washed in sterile PBS thrice. Thereafter, they were fixed in 4% paraformaldehyde at room temperature (RT) for 20min, after which they were treated with hydrogen peroxide solution (3%) to deactivate the endogenous enzymes. Subsequently, the samples were washed in PBS solution for 5 min, and then a blocking reagent (goat serum) was added at RT for 20 min after which they were incubated with primary antibody rabbit anti-ATP2B4 (Abcam, Cambridge, UK) overnight at 4℃. After the incubation process, the samples were washed and incubated again with fluorescence-labeled secondary antibody at RT for 30 min. After the second incubation process, the samples were further washed in a PBS solution and incubated again for the third time with peroxidase (POD)-labeled streptavidin (DyLight 488) at RT for 30 min. A DAB kit (BBI, Canada) was used for color development at RT for 5 ~ 30 min, which was proceeded by observation, and then photomicrographs were obtained using a light microscope (Nikon Eclipse E100, Japan) equipped with an imaging system (Nikon DS-U3, Japan). The images obtained were analyzed using Image-Pro Plus 6.0 software (Media Cybernetics, Silver Spring, USA).

Uterine tubular gland cell culture and transfection

Both ends of the uterine tissue were ligated with a cotton thread and were repeatedly dissected and cleaned with sterile Hank's balanced salt solution, thereafter the endometrial tissue was collected and cut into pieces. The cells were digested with collagenase (1 mg/mL; type I, Sigma) in a water bath at 37 ℃ for 50~60 min, and then centrifuged, after which the supernatant was discarded. This

was proceeded by resuspending the cells in a growth medium containing F12 (Hyclone) + 10% fetal bovine serum (Gibco) + 0.1% penicillin/streptomycin (Invitrogen, Carlsbad, CA, USA), and was seeded in 75 cm^2 cell culture bottles (T75) (Costar, Cambridge, MA, USA). They were then cultured in a cell culture incubator at 37 ℃, 5% CO_2, and 95% air saturated humidity for 3 h before the supernatant was filtered (using cell sieve No.200). Cell counts were performed before they were placed in a 6-well plate (1×10^6 cells/well) for further culturing [66]. We then conducted cell transfection after the cells reached a coverage density of 70–80% using lipofectamine 3000 reagent (Invitrogen, USA), according to the manufacturer's instructions. The miR-449c-5p mimic, miR-449c-5p inhibitor, mimic negative control (mimic NC), inhibitor NC, small interfering RNA (Si-ATP2B4), siRNA negative control (Si-NC), ATP2B4 overexpression plasmid (pcDNA3.1-ATP2B4), and empty pcDNA3.1 vector used in this study were designed and purchased from RiboBio (Guangzhou, China).

Immunofluorescence analysis

Immunofluorescence analysis was carried out to identify the tubular gland cells of the chicken uterus. Uterine tubular gland cells were placed in a 6-well plate, and were washed in PBS for 5min. Subsequently, the cells were fixed in 4% paraformaldehyde for 10 min and washed again; thereafter, 0.2% Triton X-100 was added to ensure permeability of the cell membrane for 10 min. The cells were washed and subsequently incubated overnight at 4℃ using primary antibody rabbit anti-Cytokertin 18 (Bioss, Beijing, China). The next morning, the cells were washed and incubated with fluorescence-labeled secondary antibody at dark room temperature for 1h. Cells were finally washed in a Tris-Buffered Saline Tween-20 (TBST) and we then observed and analyzed fluorescence intensity using a fluorescence microscope (DP80; Olympus, Japan).

Calcium ion detection in uterine tubular gland cells

The cells were cultured in 96-well plates and a calcium ion detection kit (BBcellProbe F03, BestBio Biotech Co. Ltd., Shanghai, China) was used to measure calcium ion concentration in uterine tubular gland cells following the manufacturer's instructions. BBcellProbe F03 fluorescence probe was combined with the intracellular calcium ions to produce a strong fluorescence. Values of fluorescence intensity were measured using a microplate reader (Thermo Fisher, Varioskan LUX, USA) at an excitation wavelength of 490 nm and an emission wavelength of 516 nm. Subsequently, the fields were observed and photographed using a fluorescence

417 microscope (DP80; Olympus, Japan). Three fields were randomly selected and Image-Pro plus
418 software was used for the statistical analysis.

419 **Quantitative real-time PCR (qRT-PCR)**

420 qRT-PCR analysis was conducted with a reaction volume of 10 μL containing 5 μL TB GreenTM
421 Premix (Takara), 0.5 μL forward and reverse primers, 1 μL cDNA, and 3 μL DNase/RNase-Free
422 Deionized Water (Tiangen, Beijing, China). Reaction conditions followed proper protocols and
423 instructions. Chicken GAPDH and U6 were used as internal controls. According to a gene bank,
424 the primers were designed by Oligo 6.0 software and Primer premier 5.0 software; the primers
425 used are listed in Table 1.

426 **Table 1** Primers used for qRT-PCR

Gene	Sequence (5' - 3')	Product Length (bp)	Annealing Temperature (℃)
ATP2B4	F: CCTCCGTCAATTCCACTCCC R: CTACGGAACGCATTCACCAC	89	58
GAPDH	F: TCCTCCACCTTTGATGCG R: GTGCCTGGCTCACTCCTT	146	59

427 F: Forward primer; R: Reverse primer.

428 ## Western blotting assay

429 Uterine tubular gland cells were lysed in lysis buffer (BestBio) and the total protein concentration
430 was quantified using a BCA assay (BestBio) according to the manufacturer's protocol.
431 Immunoblots were performed using prescribed primary and secondary antibodies such as
432 anti-ATP2B4 (PMCA4) (1:1000, Abcam) and goat anti-mouse IgG (Zen-Bio, Chengdu, China)
433 respectively. Western blot procedures were conducted as previously described [67].

434 ## Statistical analysis

435 Data were expressed as mean ± standard error (SE). Statistical significance was assessed by
436 one-way ANOVA followed by Duncan's multiple range tests. SAS 9.3 (SAS Inst., Cary, North
437 Carolina, USA) for Windows (GraphPad Software, San Diego, CA, USA) was used for all the
438 statistical analyses. Differences were considered significant at $P < 0.05$ (*) and $P < 0.01$ (**).

439 ## Abbreviations

440 ATP2B4: Ca^{2+}-transporting ATPase 4; SCN: suprachiasmatic nucleus; 3′ UTRs: 3′ untranslated
441 regions; miRNAs: MicroRNAs; RNA-seq: RNA sequencing; ZT: Zeitgeber time; GO: Gene

ontology; KEGG: Kyoto Encyclopedia of Genes and Genomes; DF-1: Chicken embryo fibroblast cell line; RT: Room temperature; TBST: Tris-Buffered Saline Tween-20; CK18: Cytokertin 18; PMCA4: Plasma membrane Ca^{2+}-ATPase isoform 4; ESG: Eggshell gland.

Ethics approval and consent to participate

All animal studies were approved by the Institutional Animal Care and Use Committee of Sichuan Agricultural University (Certification No. YCS-B2018102013). All experiments were carried out in compliance with the ARRIVE guidelines [68] and Sichuan Agricultural University (SAU) Laboratory Animal Welfare and Ethics guidelines.

Consent for publication

Not applicable.

Data availability statement

The data used to support the findings of this study are available from the corresponding author upon request. The raw data has been submitted to the National Center for Biotechnology Information (NCBI) Sequence Read Archive (SRA, https://submit.ncbi.nlm.nih.gov/subs/sra/); accession number (PRJNA698298).

Conflicts of interest

The authors declare that there are no conflicts of interest.

Funding

We would like to thank the China Agriculture Research System of Ministry of Agriculture and Rural Areas (Grant No. CARS-41), the National Natural Science Foundation of China (Grant No. 31872347), and The Fifth Batch of Enterprises Building Luzhou Academician Expert Workstation in 2020 for their financial support.

Authors' contributions

CZF, ZZC, and ZXL conceived and designed the experiments; CZF, ZZC, DXX, LL, TYF, and KXC performed the experiments; CZF, ZZC, AFK, SG, ZQ, WY, LDY, and ZY analyzed the data; CZF was responsible for writing the first draft of the manuscript; AFK and ZXL edited the last version of the manuscript. The final manuscript was read and approved by all authors.

Acknowledgements

We deeply appreciate Prof. Xi Peng from Department of Animal and Poultry Sciences, Chengdu University, China, for professional suggestions on this paper.

References

1. Hall JC. Genetics and molecular biology of rhythms in Drosophila and other insects. Adv Genet. 2003;**48**:1-280.
2. Reppert SM, Weaver DR. Coordination of circadian timing in mammals. Nature. 2002;**418**(6901):935-41.
3. Welsh DK, Logothetis DE, Meister M, Reppert SM. Individual neurons dissociated from rat suprachiasmatic nucleus express independently phased circadian firing rhythms. Neuron. 1995;**14**(4):697-706.
4. Pevet P, Challet E. Melatonin: both master clock output and internal time-giver in the circadian clocks network. J Physiol Paris. 2011;**105**(4-6):170-82.
5. Mohawk JA, Green CB, Takahashi JS. Central and peripheral circadian clocks in mammals. Annu Rev Neurosci. 2012;**35**:445-62.
6. Bell-Pedersen D, Cassone VM, Earnest DJ, Golden SS, Hardin PE, Thomas TL, Zoran MJ. Circadian rhythms from multiple oscillators: lessons from diverse organisms. Nat Rev Genet. 2005;**6**(7):544-56.
7. Lowrey PL, Takahashi JS. Genetics of circadian rhythms in Mammalian model organisms. Adv Genet. 2011;**74**:175-230.
8. Albrecht U. Timing to perfection: the biology of central and peripheral circadian clocks. Neuron. 2012;**74**(2):246-60.
9. Gekakis N, Staknis D, Nguyen HB, Davis FC, Wilsbacher LD, King DP, Takahashi JS, Weitz CJ. Role of the CLOCK protein in the mammalian circadian mechanism. Science. 1998;**280**(5369):1564-9.
10. Yoo SH, Ko CH, Lowrey PL, Buhr ED, Song EJ, Chang S, Yoo OJ, Yamazaki S, Lee C, Takahashi JS. A noncanonical E-box enhancer drives mouse Period2 circadian oscillations in vivo. Proc Natl Acad Sci U S A. 2005;**102**(7):2608-13.
11. Kiyohara YB, Nishii K, Ukai-Tadenuma M, Ueda HR, Uchiyama Y, Yagita K. Detection of a circadian enhancer in the mDbp promoter using prokaryotic transposon vector-based strategy. Nucleic Acids Res. 2008;**36**(4):e23.
12. Kumaki Y, Ukai-Tadenuma M, Uno KD, Nishio J, Masumoto KH, Nagano M, Komori T, Shigeyoshi Y, Hogenesch JB, Ueda HR. Analysis and synthesis of high-amplitude Cis-elements in the mammalian circadian clock. Proc Natl Acad Sci U S A. 2008;**105**(39):14946-51.
13. Hardin PE. Transcription regulation within the circadian clock: the E-box and beyond. J Biol Rhythms. 2004;**19**(5):348-60.
14. Lowrey PL, Takahashi JS. Mammalian circadian biology: elucidating genome-wide levels of temporal organization. Annu Rev Genomics Hum Genet. 2004;**5**:407-41.
15. Hastings MH, Reddy AB, Maywood ES. A clockwork web: circadian timing in brain and periphery, in health and disease. Nat Rev Neurosci. 2003;**4**(8):649-61.
16. Panda S, Hogenesch JB. It's all in the timing: many clocks, many outputs. J Biol Rhythms. 2004;**19**(5):374-87.
17. Yoshitane H, Ozaki H, Terajima H, Du NH, Suzuki Y, Fujimori T, Kosaka N, Shimba S, Sugano S, Takagi T, Iwasaki W, Fukada Y. CLOCK-controlled polyphonic regulation of circadian rhythms through canonical and noncanonical E-boxes. Mol Cell Biol. 2014;**34**(10):1776-87.

18. Hardin PE, Panda S. Circadian timekeeping and output mechanisms in animals. Curr Opin Neurobiol. 2013;**23**(5):724-31.
19. Kondratov RV, Kondratova AA, Lee C, Gorbacheva VY, Chernov MV, Antoch MP. Post-translational regulation of circadian transcriptional CLOCK(NPAS2)/BMAL1 complex by CRYPTOCHROMES. Cell Cycle. 2006;**5**(8):890-5.
20. Dibner C, Schibler U, Albrecht U. The mammalian circadian timing system: organization and coordination of central and peripheral clocks. Annu Rev Physiol. 2010;**72**:517-49.
21. Landgraf D, Wang LL, Diemer T, Welsh DK. NPAS2 Compensates for Loss of CLOCK in Peripheral Circadian Oscillators. PLoS Genet. 2016;**12**(2):e1005882.
22. DeBruyne JP, Weaver DR, Reppert SM. CLOCK and NPAS2 have overlapping roles in the suprachiasmatic circadian clock. Nat Neurosci. 2007;**10**(5):543-5.
23. Debruyne JP, Noton E, Lambert CM, Maywood ES, Weaver DR, Reppert SM. A clock shock: mouse CLOCK is not required for circadian oscillator function. Neuron. 2006;**50**(3):465-77.
24. Englund A, Kovanen L, Saarikoski ST, Haukka J, Reunanen A, Aromaa A, Lönnqvist J, Partonen T. NPAS2 and PER2 are linked to risk factors of the metabolic syndrome. J Circadian Rhythms. 2009;**7**:5.
25. Du T, Zamore PD. microPrimer: the biogenesis and function of microRNA. Development. 2005;**132**(21):4645-52.
26. He L, Hannon GJ. MicroRNAs: small RNAs with a big role in gene regulation. Nat Rev Genet. 2004;**5**(7):522-31.
27. Xu S, Witmer PD, Lumayag S, Kovacs B, Valle D. MicroRNA (miRNA) transcriptome of mouse retina and identification of a sensory organ-specific miRNA cluster. J Biol Chem. 2007;**282**(34):25053-66.
28. Zhang W, Wang P, Chen S, Zhang Z, Liang T, Liu C. Rhythmic expression of miR-27b-3p targets the clock gene Bmal1 at the posttranscriptional level in the mouse liver. FASEB J. 2016;**30**(6):2151-60.
29. Zhou W, Li Y, Wang X, Wu L, Wang Y. MiR-206-mediated dynamic mechanism of the mammalian circadian clock. BMC Syst Biol. 2011;**5**:141.
30. Cheng HY, Papp JW, Varlamova O, Dziema H, Russell B, Curfman JP, Nakazawa T, Shimizu K, Okamura H, Impey S, Obrietan K. microRNA modulation of circadian-clock period and entrainment. Neuron. 2007;**54**(5):813-29.
31. Tan X, Zhang P, Zhou L, Yin B, Pan H, Peng X. Clock-controlled mir-142-3p can target its activator, Bmal1. BMC Mol Biol. 2012;**13**:27.
32. Yang M, Lee JE, Padgett RW, Edery I. Circadian regulation of a limited set of conserved microRNAs in *Drosophila*. BMC Genomics. 2008;**9**:83.
33. Chen W, Liu Z, Li T, Zhang R, Xue Y, Zhong Y, Bai W, Zhou D, Zhao Z. Regulation of Drosophila circadian rhythms by miRNA let-7 is mediated by a regulatory cycle. Nat Commun. 2014;**5**:5549.
34. Saus E, Soria V, Escaramís G, Vivarelli F, Crespo JM, Kagerbauer B, Menchón JM, Urretavizcaya M, Gratacòs M, Estivill X. Genetic variants and abnormal processing of pre-miR-182, a circadian clock modulator, in major depression patients with late insomnia. Hum Mol Genet. 2010;**19**(20):4017-25.
35. Jacovetti C, Rodriguez-Trejo A, Guay C, Sobel J, Gattesco S, Petrenko V, Saini C, Dibner C, Regazzi R. MicroRNAs modulate core-clock gene expression in pancreatic islets during early

postnatal life in rats. Diabetologia. 2017;**60**(10):2011-2020.
36. Brandstätter R, Abraham U. Hypothalamic circadian organization in birds. I. Anatomy, functional morphology, and terminology of the suprachiasmatic region. Chronobiol Int. 2003;**20**(4):637-55.
37. Gwinner E, Hau M, Heigl S. Melatonin: generation and modulation of avian circadian rhythms. Brain Res Bull. 1997;**44**(4):439-44.
38. Cassone VM, Takahashi JS, Blaha CD, Lane RF, Menaker M. Dynamics of noradrenergic circadian input to the chicken pineal gland. Brain Res. 1986;**384**(2):334-41.
39. Chong NW, Chaurasia SS, Haque R, Klein DC, Iuvone PM. Temporal-spatial characterization of chicken clock genes: circadian expression in retina, pineal gland, and peripheral tissues. J Neurochem. 2003;**85**(4):851-60.
40. Tischkau SA, Howell RE, Hickok JR, Krager SL, Bahr JM. The luteinizing hormone surge regulates circadian clock gene expression in the chicken ovary. Chronobiol Int. 2011;**28**(1):10-20.
41. Zhang ZC, Wang YG, Li L, Yin HD, Li DY, Wang Y, Zhao XL, Liu YP, Zhu Q. Circadian clock genes are rhythmically expressed in specific segments of the hen oviduct. Poult Sci. 2016;**95**(7):1653-1659.
42. Marie P, Labas V, Brionne A, Harichaux G, Hennequet-Antier C, Nys Y, Gautron J. Data set for the proteomic inventory and quantitative analysis of chicken uterine fluid during eggshell biomineralization. Data Brief. 2014;**1**:65-9.
43. Huang JE, Huang QY, Chen WP, Liang ZD. Protective effects of bFGF on rats'renal tubular epithelial cells damaged by gentamicin in vitro. Chin Pharmacol Bull. 2005; **21**(2):232-5.
44. Moll R, Franke WW, Schiller DL, Geiger B, Krepler R. The catalog of human cytokeratins: patterns of expression in normal epithelia, tumors and cultured cells. Cell. 1982;**31**(1):11-24.
45. Rodríguez-Navarro AB, Marie P, Nys Y, Hincke MT, Gautron J. Amorphous calcium carbonate controls avian eggshell mineralization: A new paradigm for understanding rapid eggshell calcification. J Struct Biol. 2015;**190**(3):291-303.
46. Jonchère V, Brionne A, Gautron J, Nys Y. Identification of uterine ion transporters for mineralisation precursors of the avian eggshell. BMC Physiol. 2012;**12**:10.
47. Nys YM, Hincke MT, Arias JL, Garcia-Ruiz JM, Solomon SE. Avian eggshell mineralization. Poult Avian Biol Rev. 1999;**10**(3):143-66.
48. Xu R, Zhao M, Yang Y, Huang Z, Shi C, Hou X, Zhao Y, Chen B, Xiao Z, Liu J, Miao Q, Dai J. MicroRNA-449c-5p inhibits osteogenic differentiation of human VICs through Smad4-mediated pathway. Sci Rep. 2017;**7**(1):8740.
49. Parker SL, Lindsay LA, Herbert JF, Murphy CR, Thompson MB. Expression and localization of Ca^{2+}-ATPase in the uterus during the reproductive cycle of king quail (Coturnix chinensis) and zebra finch (Poephila guttata). Comp Biochem Physiol A Mol Integr Physiol. 2008;**149**(1):30-5.
50. Tempel BL, Shilling DJ. The plasma membrane calcium ATPase and disease. Subcell Biochem. 2007;**45**:365-83.
51. Hodges RD, Lrcher K. Possible sources of the carbonate fraction of egg shell calcium carbonate. Nature. 1967;**216**(5115):609-10.
52. Lippiello L, Wasserman RH. Fluorescent antibody localization of the vitamin D-dependent calcium-binding protein in the oviduct of the laying hen. J Histochem Cytochem.

1975;**23**(2):111-6.
53. Coty WA, Mc Conkey CL Jr. A high-affinity calcium-stimulated ATPase activity in the hen oviduct shell gland. Arch Biochem Biophys. 1982;**219**(2):444-53.
54. Bar A. Calcium transport in strongly calcifying laying birds: mechanisms and regulation. Comp Biochem Physiol A Mol Integr Physiol. 2009;**152**(4):447-69.
55. Pike JW, Alvarado RH. Ca-2+-Mg-2+-activated ATPase in the shell gland of japanese quail (Coturnix coturnix japonica). Comp Biochem Physiol B. 1975;**51**(1):119-25.
56. Wasserman RH, Smith CA, Smith CM, Brindak ME, Fullmer CS, Krook L, Penniston JT, Kumar R. Immunohistochemical localization of a calcium pump and calbindin-D28k in the oviduct of the laying hen. Histochemistry. 1991;**96**(5):413-8.
57. Lundholm CD. DDE-induced eggshell thinning in birds: effects of p,p'-DDE on the calcium and prostaglandin metabolism of the eggshell gland. Comp Biochem Physiol C Pharmacol Toxicol Endocrinol. 1997;**118**(2):113-28.
58. Bozgeyik E, Arman K, Igci YZ. ATP2B4 (ATPase, Ca++ transporting, plasma membrane 4). Atlas of Genetics and Cytogenetics in Oncology and Haematology. 2017.
59. Strehler EE, Zacharias DA. Role of alternative splicing in generating isoform diversity among plasma membrane calcium pumps. Physiol Rev. 2001;**81**(1):21-50.
60. Hoenderop JG, Nilius B, Bindels RJ. Calcium absorption across epithelia. Physiol Rev. 2005;**85**(1):373-422.
61. Stokes DL, Green NM. Structure and function of the calcium pump. Annu Rev Biophys Biomol Struct. 2003;**32**:445-68.
62. Hughes ME, Hogenesch JB, Kornacker K. JTK_CYCLE: an efficient nonparametric algorithm for detecting rhythmic components in genome-scale data sets. J Biol Rhythms. 2010;**25**(5):372-80.
63. Liu L, Xiao Q, Gilbert ER, Cui Z, Zhao X, Wang Y, Yin H, Li D, Zhang H, Zhu Q. Whole-transcriptome analysis of atrophic ovaries in broody chickens reveals regulatory pathways associated with proliferation and apoptosis. Sci Rep. 2018;**8**(1):7231.
64. Friedman RC, Farh KK, Burge CB, Bartel DP. Most mammalian mRNAs are conserved targets of microRNAs. Genome Res. 2009;**19**(1):92-105.
65. Shannon P, Markiel A, Ozier O, Baliga NS, Wang JT, Ramage D, Amin N, Schwikowski B, Ideker T. Cytoscape: a software environment for integrated models of biomolecular interaction networks. Genome Res. 2003;**13**(11):2498-504.
66. Muramatsu T, Hiramatsu H, Okumura J. Induction of ovalbumin mRNA by ascorbic acid in primary cultures of tubular gland cells of the chicken oviduct. Comp Biochem Physiol B Biochem Mol Biol. 1995;**112**(2):209-16.
67. Cui Z, Liu L, Kwame Amevor F, Zhu Q, Wang Y, Li D, Shu G, Tian Y, Zhao X. High Expression of miR-204 in Chicken Atrophic Ovaries Promotes Granulosa Cell Apoptosis and Inhibits Autophagy. Front Cell Dev Biol. 2020;**8**:580072.
68. Percie du Sert N, Ahluwalia A, Alam S, Avey MT, Baker M, Browne WJ, Clark A, Cuthill IC, Dirnagl U, Emerson M, Garner P, Holgate ST, Howells DW, Hurst V, Karp NA, Lazic SE. Reporting animal research: Explanation and elaboration for the ARRIVE guidelines 2.0. PLoS Biol. 2020;**18**(7):e3000411.

Figures

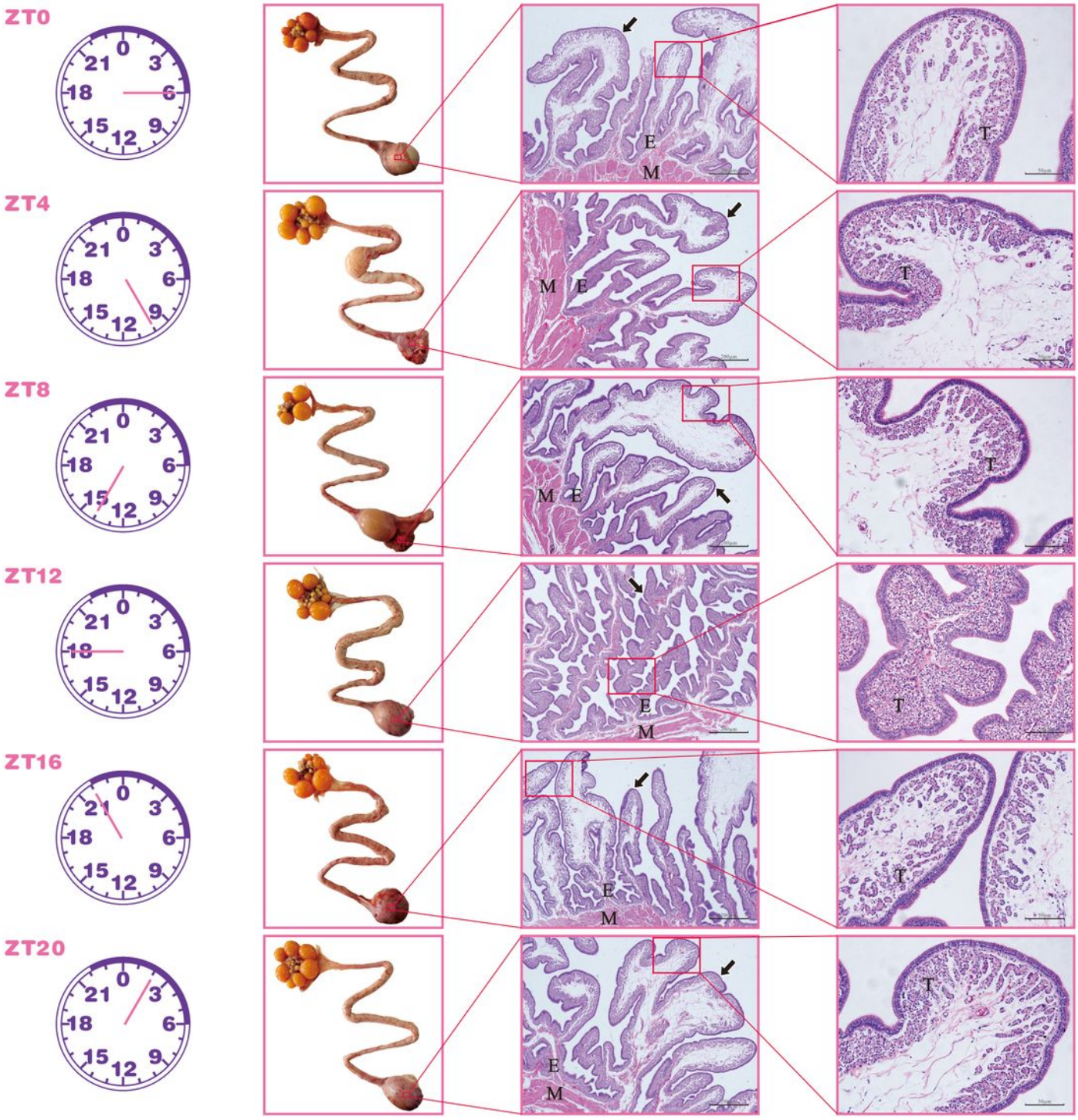

Figure 1

Chicken uterus morphological and histological characteristics. Hematoxylin eosin (H&E) staining of chicken uterus at ZT4, ZT8, ZT12, ZT16, ZT20, and ZT0 (ZT24), respectively (magnified 200×).

Replications = 3. E: endometrium; M: myometrium; T: tubular gland cells. The black arrow indicates the endometrial glands.

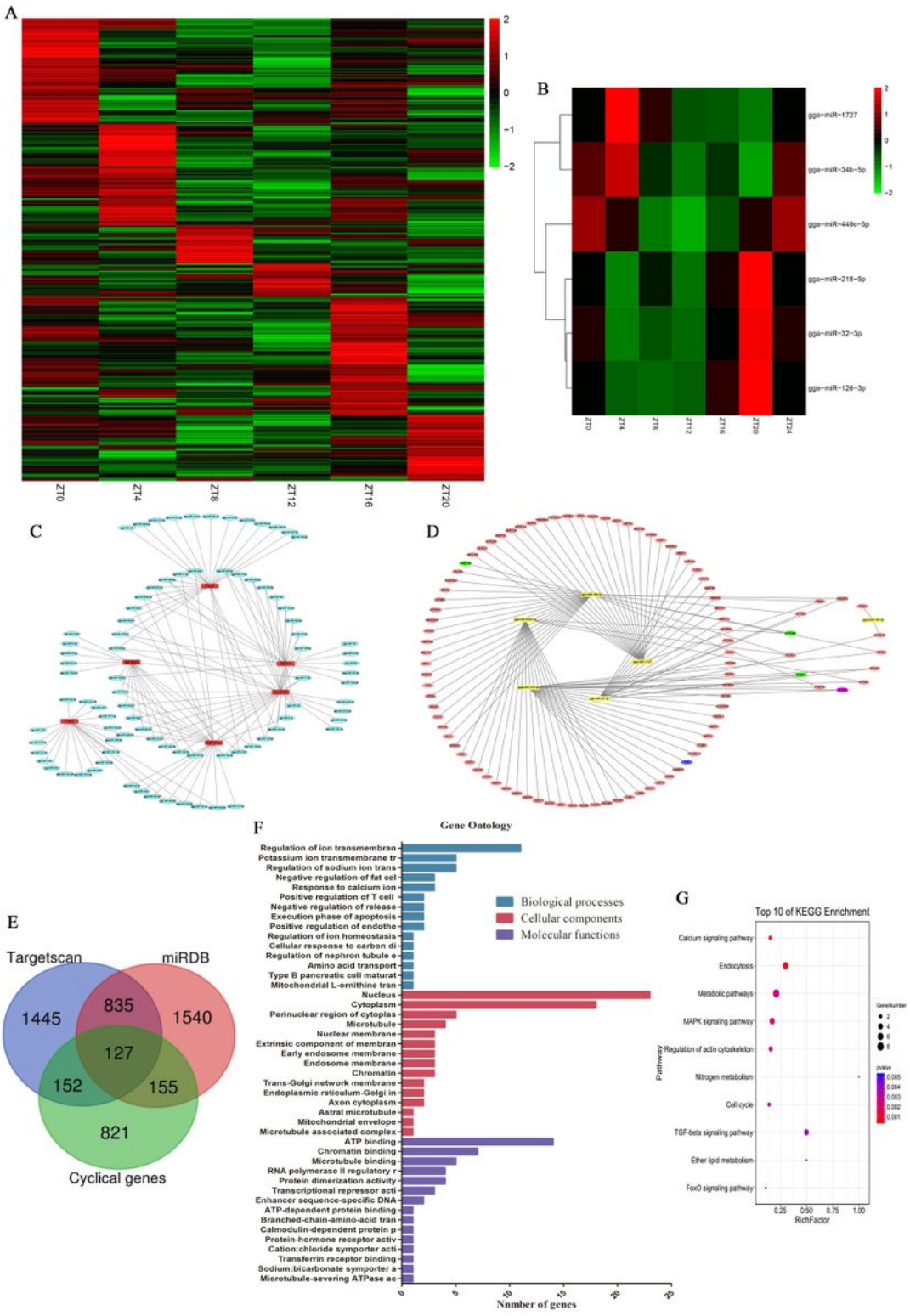

Figure 2

Identification of circadian miRNAs and functional analysis. (A) Heatmap of a total of 375 miRNAs in chicken uterus at ZT4, ZT8, ZT12, ZT16, ZT20, and ZT0 (ZT24) within 24 h. (B) Heatmap of six circadian miRNAs. (C) Core clock genes miRNAs correlation netwo rk in chicken uterus. (D) Circadian miRNAs

target genes correlation network in chicken uterus. (E) Venn diagram showing the target genes of six circadian miRNAs using Targetscan and miRDB software, and uterine cyclical genes. (F) GO enrichment of the 127 c ircadian target genes. Top 15 terms of biological process, cellular component, and molecular function. X axis shows the number of genes. (G) Top 10 significantly enriched pathways associated with 127 circadian target genes.

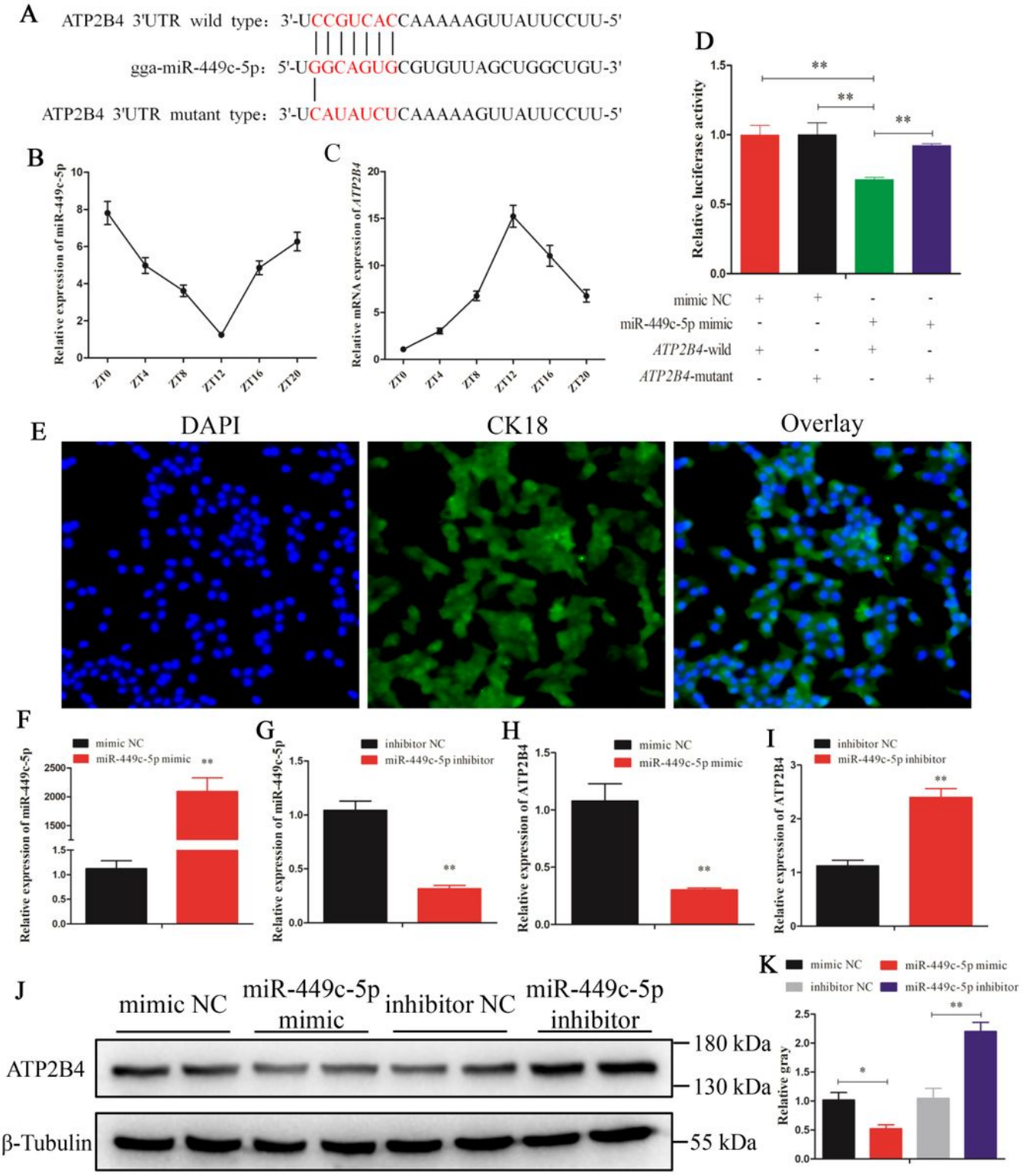

Figure 3

targeting ATP2B4 in uterine tubular gland cells. (A) The target position of the miR 449c 5p seed sequence on the gene ATP2B4 3'UTR sequence (red characters) was predicte d by TargetScan software. (B, C) Relative expression of miR 449c 5p and ATP2B4 at the time point of ZT0 (ZT24), ZT4, ZT8, ZT12, ZT16, and ZT20 in chicken uterus, respectively. (D) Chicken DF 1 cells were co transfected with ATP2B4 3 UTR wild or mutant dual luciferase vector and the miR 449c 5p mimic or mimic NC. The relative luciferase activity was assayed 48h later. (E) Immunofluorescence analysis was performed to identify the uterine tubular gland cells. (F, G) qRT PCR was used to determine the miR 449c 5 p expression levels after transfection of 169 miR 449c 5p overexpression and miR 449c 5p inhibition plasmid, respectively. (H, I) mRNA expression of ATP2B4 in chicken uterine tubular gland cells was detected by qRT PCR after overexpression and inhibition of mi R 449c 5p, respectively. (J, K) Protein expression of ATP2B4 in chicken uterine tubular gland cells was detected by Western blot analysis after a gain or loss of miR 449c 5p, respectively. UTR: untranslated region; miR: microRNA; DAPI: 4', 6 diamidino 2 ph enylindole; NC: negative control. Replications = 3. The samples derive from the same experiment and that gels/blots were processed in parallel The data is presented as mean ± 176 standard error (SE); * P < 0.05 and P <0.01

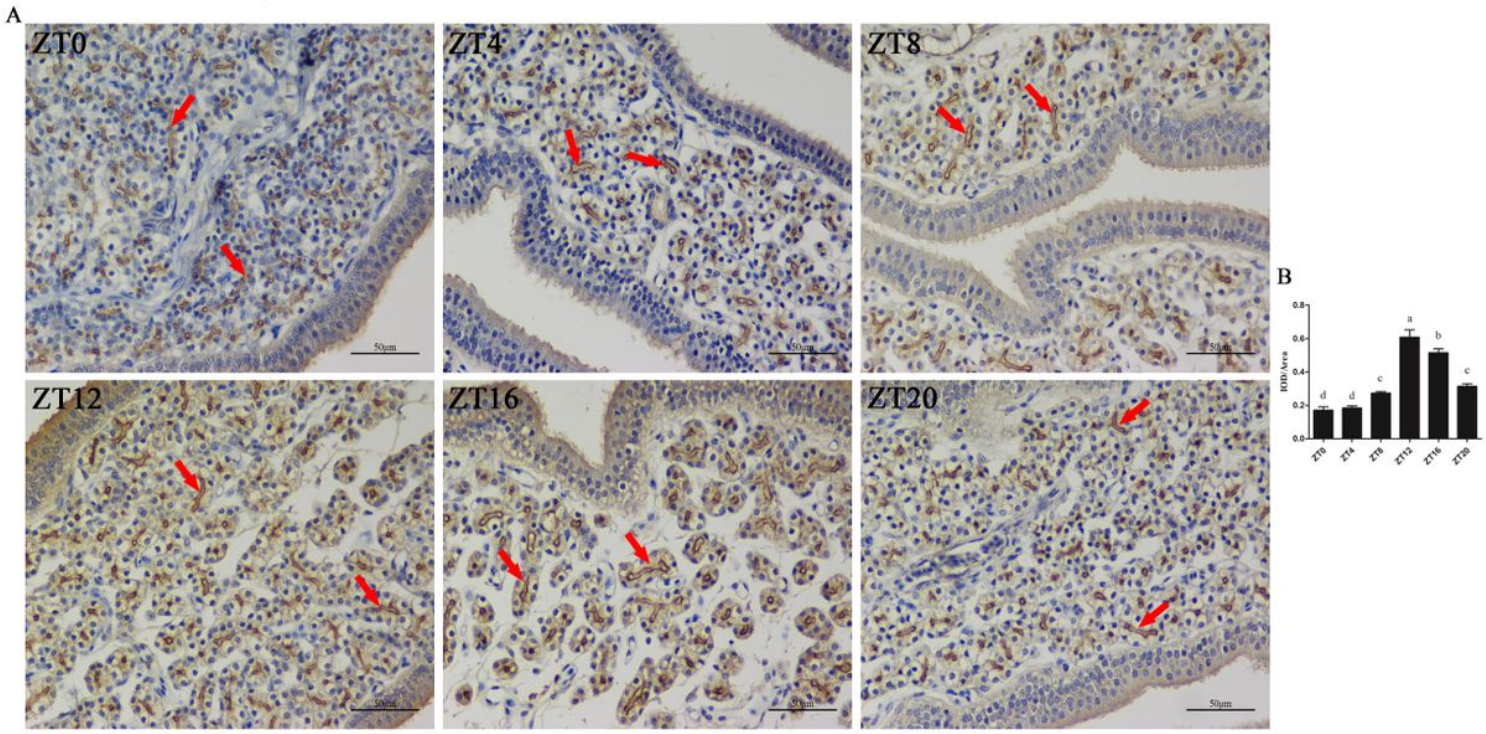

Figure 4

ATP2B4 immunohistochemistry in the chicken uterus. (A) Immunohistochemical staining with the ATP2B4 antibody visualized using chromogen diaminobenzene (brown staining) in the chicken uterus. Arrows indicate the relative areas of positive staining. (B) Dig ital conversion histogram; each point represents the mean ± SE. Different lowercase letters indicate a significant difference among groups (P < 0.05)

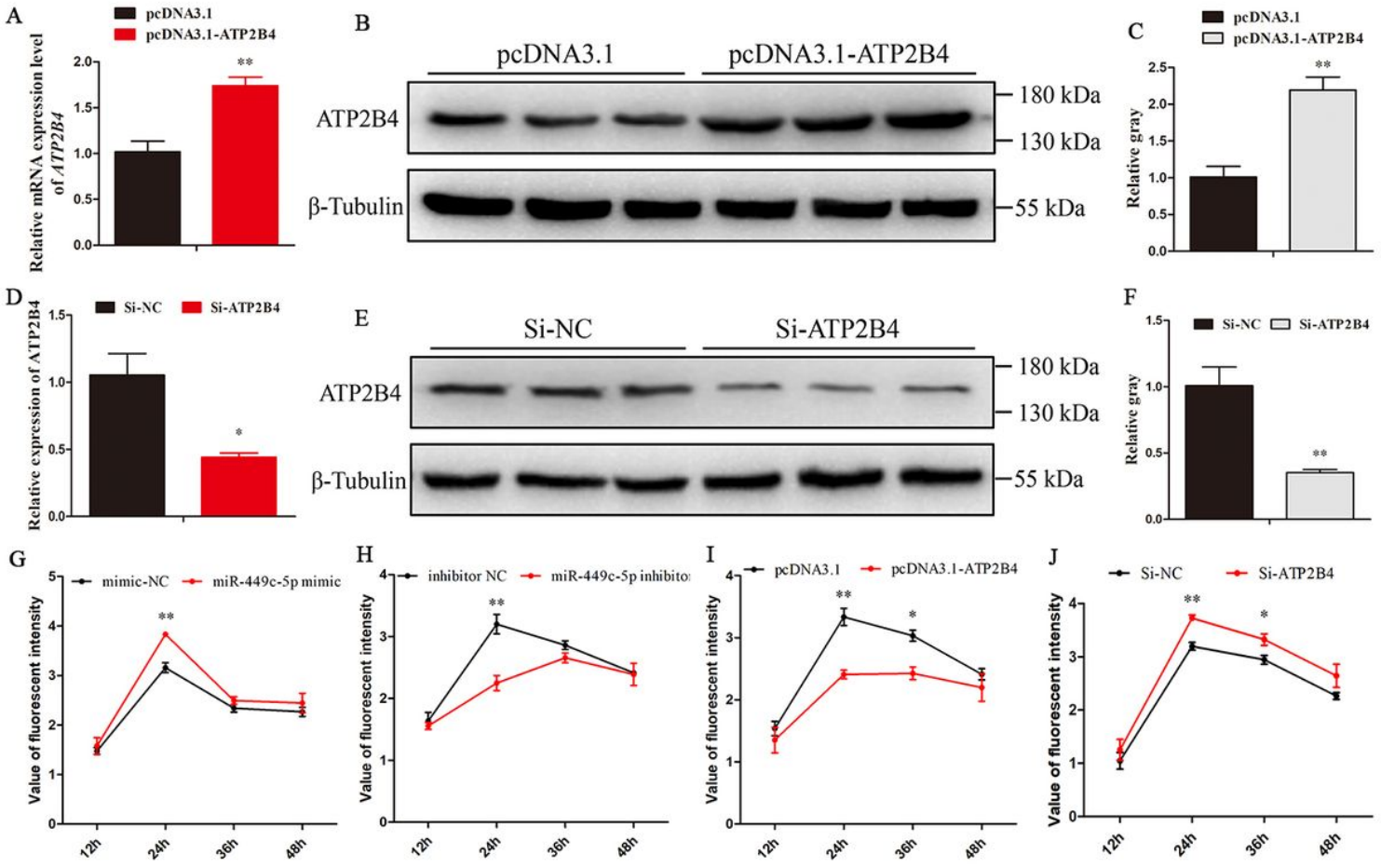

Figure 5

ATP2B4 regulated Ca 2+ transfer in uterine tubular gland cells. (A, B and C) mRNA and protein expressions of ATP2B4 were detected after transfection of overexpression plasmid (pcDNA3.1 ATP2B4) and empty pcDNA3.1 vector. (D, E, and F) mRNA and protein expressions of ATP2B4 were detected after transfection of small interfering RNA (Si ATP2B4) and siRNA negative control (Si NC). (G and H) Value of fluorescen t intensity was measured using a microplate reader indicating the intracellular concentration of Ca 2+ after overexpression and inhibition of miR 449c 5p. (I and J) The intracellular concentration of Ca 2+ ion was detected after transfection overexpression a nd inhibition of ATP2B4. Replications = 3. The samples derive from the same experiment and that gels/blots were processed in parallel. Data are presented as mean ± standard error (SE); * $P < 0.05$ and $P < 0.01$.

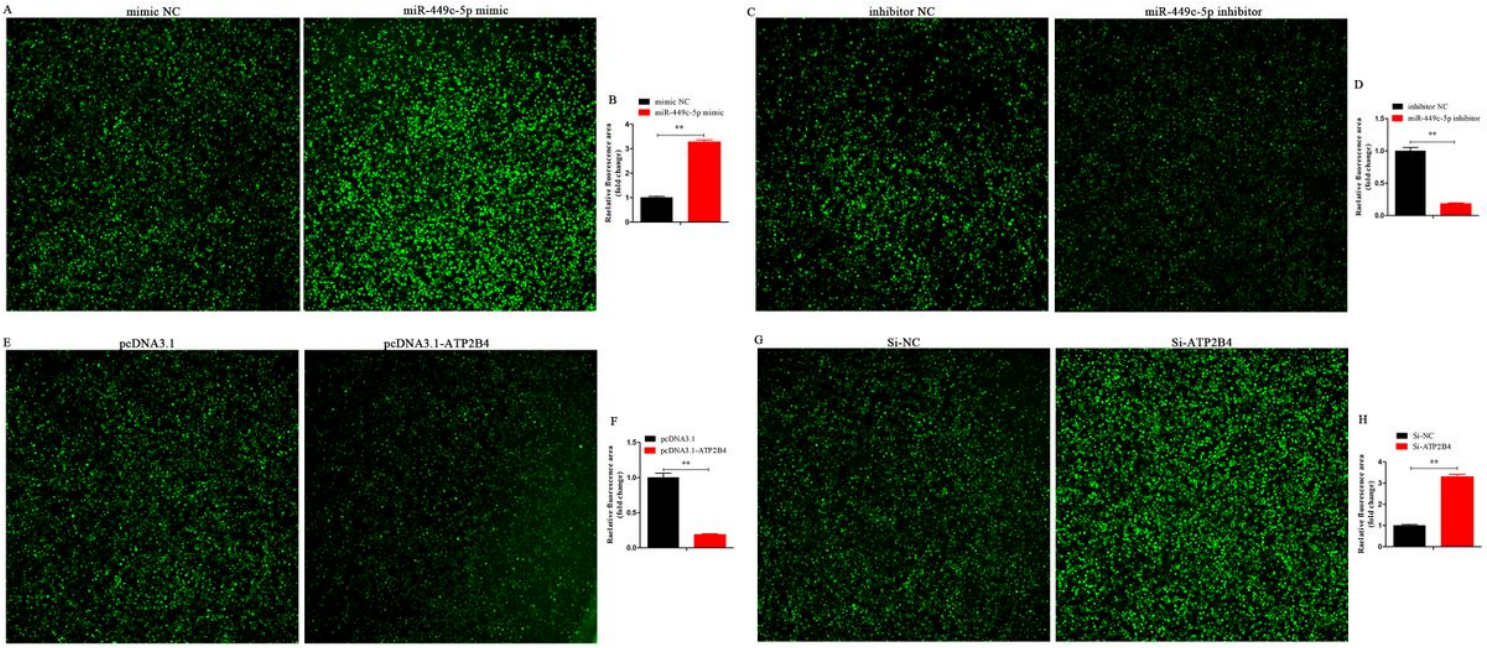

Figure 6

Clock controlled miR 449c 5p regulated Ca 2+ transport by targeting ATP2B4 in chicken uterine tubular gland cells. (A and B) Fluorescence intensity was observed and analyzed after overexpression of miR 449c 5p. (C and D) Fluorescence intensity was observed and analyzed after inhibition of miR 449c 5p. (E, F, G, and H) Fluorescence intensity was observed and analyzed after transfection, overexpression, and inhibition of ATP2B4. Replications = 3. Data are presented as mean ± standard error (SE); * $P < 0.05$ and $P < 0.01$.

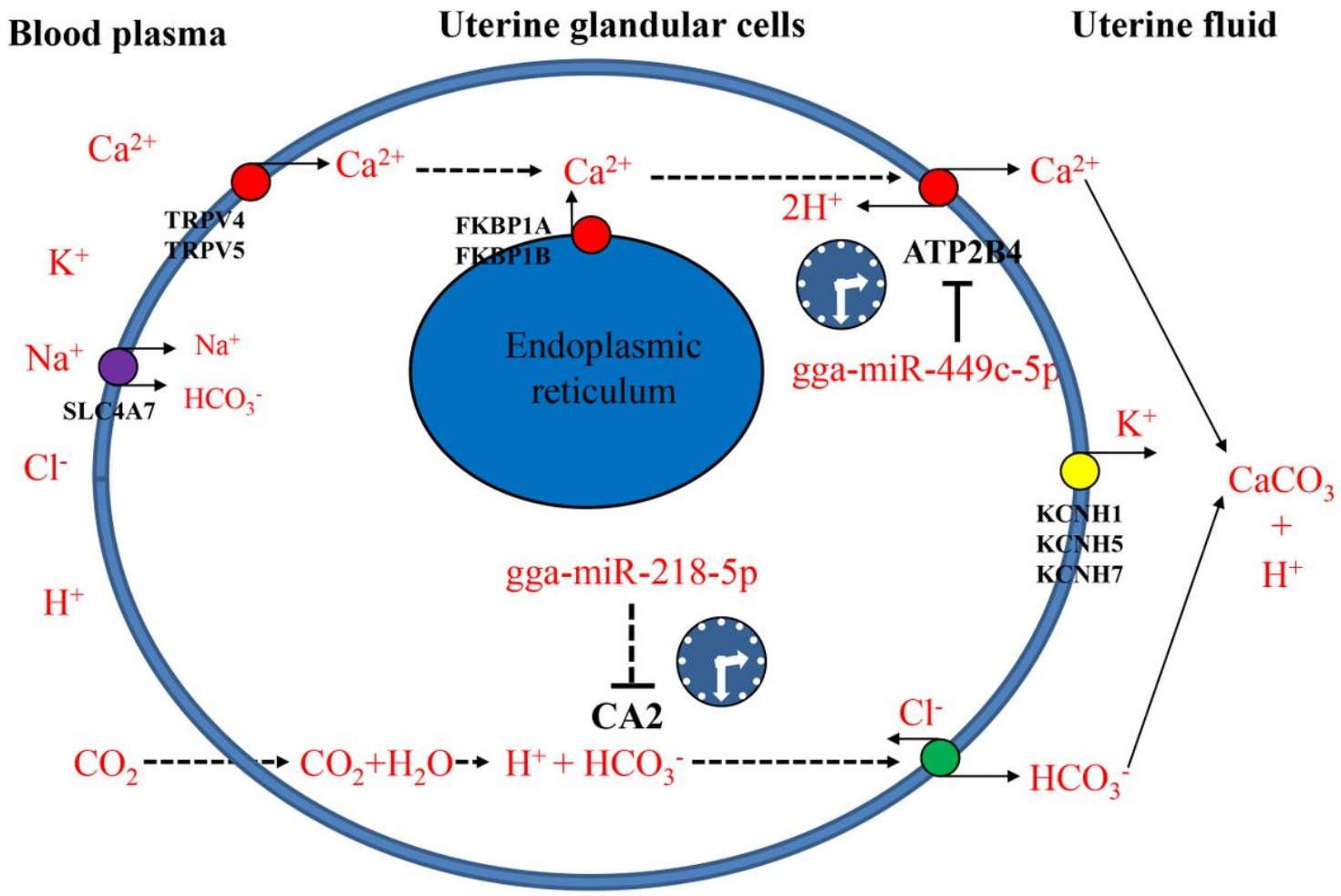

Figure 7

The general model describing clock controlled miRNA regulated ion transporters during eggshell calcification in the chicken uterus. This figure summarizes the general mechanisms involved in the regulation of the transport, distribution, and transformation of Ca 2+ from the blood plasma through the uterine tubular gland cell membrane (Ca 2+ trans epithelial transport) and then suspended in the uterine fluid in a usable form (CaCO 3) to be utilized in eggshell calcification. Clock controlled miR 449c 5p in the uterus of chickens regulated Ca 2+ transport by targeting ATP2B4 during eggshell calcification. ATP2B4 was responsible for utilizing the stored energy in the form of ATP to extrude Ca 2+ out of the cell against the electrochemical gradient and it was also involved in the active transport of calcium out of the tubular gland cells into the calcium rich fluid of the uterine lumen. NPAS2 , one of the core clock genes, was predicted to be the target gene of clock controlled miR 218 5p, and another target gene CA2 , was related to the carbonic anhydrase activity of the hen oviduct.

Supplementary Files

This is a list of supplementary files associated with this preprint. Click to download.

- SupplementaryInformation.pdf